X-ray diffraction study of the static strength of tungsten to 69 GPa

Duanwei He* and Thomas S. Duffy
Department of Geosciences, Princeton University, Princeton, New Jersey 08544, USA
(Received 1 December 2005; revised manuscript received 9 February 2006; published 12 April 2006)

The strength of tungsten was determined under static high pressures to 69 GPa using x-ray diffraction techniques in a diamond anvil cell. Analysis of x-ray diffraction peak broadening and measurement of peak shifts associated with lattice strains are two different methods for strength determination of materials under large nonhydrostatic compressions. Here these methods are directly compared under uniaxial compression in a diamond anvil cell. Our results demonstrate the consistency of the two approaches, and show that the yield strength of tungsten increases with compression, reaching a value of 5.3 GPa at the highest pressure. The obtained yield strength of tungsten is also compared with previous experimental data involving shock wave and static compression measurements, and with theoretical predictions. The high-pressure strength of tungsten is comparable to that of other dense metals such as Re and Mo, and ratio of yield strength to shear modulus is about 0.02 for all these materials between 20 and 70 GPa. The static strength of tungsten is much greater than values observed for W under shock loading but is very similar to values observed under quasi-isentropic loading.

DOI: 10.1103/PhysRevB.73.134106 PACS number(s): 62.50.+p, 64.10.+h, 62.20.Fe, 61.10.Nz

INTRODUCTION

Bcc transition metals such as tungsten are technologically important materials. The mechanical behavior of these metals under high static pressures has been a subject of interest since the pioneering work of Bridgman.[1–3] The strength properties of incompressible metals (e.g., W, Re) are of considerable importance for optimizing the design and operation of high-pressure apparatus.[4,5] Pressure calibration in diamond anvil cells is largely based on equations of state derived from shock data for standard materials such as W, Mo, Cu, etc.[6–8] In the reduction of shock compression data, strength differences between static data and Hugoniot states have generally been neglected, but these could be a significant source of error in diamond anvil cell experiments when the pressure is not hydrostatic.[6,8] The static strength in a given experiment may depend on the pressure environment which can range from hydrostatic (fluid pressure-transmitting medium) to quasihydrostatic (soft medium) to nonhydrostatic (no medium). Here we use nonhydrostatic compression to determine the maximum static strength of W and directly compare static and shock strengths to high pressures.

The gasketed diamond anvil pressure cell can generate a uniaxial stress field at the center of the sample under nonhydrostatic compression. According to the lattice strain theory developed by Singh *et al.*,[9–12] the slope of the relation between measured lattice strain and the angle ψ between the diffraction vector and the loading axis of the cell is directly related to the ratio t/G, where t is the mean differential stress and G is the shear modulus. If the macroscopic differential stress t has reached its limiting value (the yield strength) at high pressures, t/G will reflect the ratio of yield strength to shear modulus. Combined with independent constraints on the high-pressure shear modulus, the differential stress or yield strength at high pressure can be determined. Radial x-ray diffraction techniques together with the lattice strain theory have been applied to strength determination of many materials.[5,13–20]

Microscopic deviatoric stress also exists in a polycrystalline sample under nonhydrostatic compression caused by grain-to-grain contact and/or strength of the pressure medium. The magnitude and orientation of this stress field generally is distributed randomly, and leads to broadening of diffraction peaks. The amount of broadening due to lattice distortion yields a measure of the microscopic deviatoric strain distribution ε parallel to the diffraction vector. The microscopic deviatoric stress v can be determined by multiplying ε by the aggregate high-pressure Young's modulus E. If sufficient deviatoric stress is generated to deform the sample plastically, then this stress also represents the yield strength of the sample.[21] Analysis of the diffraction peak broadening also has been used to determine the yield strength for many materials using multi-anvil apparatus.[21–25] In fact, the above two methods are both frequently used to investigate the strength of materials under large nonhydrostatic compression. In principle, they should give the same result, as both the macroscopic differential stress t and microscopic deviatoric stress v that the sample can support should be equal to the yield strength once the plastic deformation is initialized.[18] Therefore, it is of interest to critically compare these two methods under the same stress conditions and for the same material.

In this study, the yield strength of a polycrystalline tungsten sample was investigated using radial x-ray diffraction techniques under uniaxial compression up to 68.8 GPa. In addition to its technological importance, tungsten was chosen for study because of its strong x-ray diffraction signal and high yield strength, and because its elastic properties and strength have been widely examined in previous dynamic and static compression experiments.[1,5,8,26–36]

EXPERIMENT

Tungsten powder (Alfa, 99.999%, 4–6 μm grain size) was loaded into a 90-μm-diameter hole of a Be gasket in a

diamond anvil cell. The gasket was preindented to 28 μm thickness at 23 GPa. A piece of ~40 μm Au foil was placed on top of the sample and served as a pressure standard.[37] We used a symmetric diamond anvil cell with a culet size of 300 μm to exert uniaxial compression on both the W sample and Au. No pressure-transmitting medium was used. Energy-dispersive radial x-ray diffraction experiments[18,38] were performed at X17C beamline of the National Synchrotron Light Source at Brookhaven National Laboratory. Two pairs of slits are positioned in the diffracted beam path. One slit determines the angular resolution of the system and the other slit defines the spatial region from which diffracted intensity is collected. This spatial resolution is an advantage for radial geometry experiments as diffracted intensity can be restricted to regions near the loading axis where the lattice strain equations strictly apply.[18] The incident x-ray beam was focused by a pair of Kirkpatrick-Baez mirrors to approximately 10×15 μm^2 and directed through the Be gasket and the sample. The diffracted intensity was recorded using a Ge solid-state detector with a fixed angle at $2\theta=12.004(4)°$ which was calibrated with a separate gold foil.

The diamond cell was mounted in a rotation stage whose axis bisects 2θ. Thus the angle ψ between the diffraction plane normal and the cell-loading axis could vary from 0° (diffraction normal parallel to the diamond cell loading axis) to 90° (diffraction normal perpendicular to the loading axis). A detailed description of the experimental setup is provided elsewhere.[13,14,18] Before data collection, the cell was scanned in the horizontal and vertical directions while recording x-ray transmission with a photodiode to determine the appropriate sample position. Diffraction spectra were collected only after sufficient time (more than 1 h) elapsed after each compression step to allow for stress relaxation. A total of 12 pressure steps were investigated. For seven of the pressure steps, diffraction patterns were taken at $\psi=0°$, 20°, 28°, 35°, 42°, 50°, 54.7°, 60°, 70°, and 90°, respectively. For the rest of the pressure steps, patterns were collected only at $\psi=0°$, 54.7°, and 90°. The diffraction patterns obtained at $\psi>60°$ were excluded from data analysis to avoid the systematic error due to the strong x-ray absorption of W,[39] and positioning errors that were detected only after data collection was completed. However, the d spacing vs angle trend is well defined by data between 0°-60°.

For data taken at higher pressures, we always rotated the stage back to $\psi=0°$ and collected data again to compare with the patterns taken at the beginning of the data collection step. The variation in d spacing at $\psi=0°$ was typically less than 0.2% over the measurement time interval and not systematic.[18] At four of the loading steps, diffraction patterns were also collected along a linear transect across the sample surface at 10 μm steps at $\psi=0°$. The variation in pressure measured over the central 40 μm was approximately 5%. With the diamond cell oriented at $\psi=0°$, we also carried out a transect along the loading axis (at right angles to the diamond surface) and found no detectable change in the diffraction peak positions for Au or W with distance from the diamond surface.

Peak position and width (full width at half maximum) were obtained by fitting background-subtracted Voigt line shapes to the spectra. The lattice parameters of Au were derived from the (111), (200), (220), (311), and (222) diffraction lines. Hydrostatic pressures were obtained from the mean lattice parameter of gold at $\psi=54.7°$. As reported previously,[13,14] the (200) diffraction line of gold is anomalous. This may be a consequence of plastic deformation.[23,40] However, the effect of including or excluding (200) on pressure determination was small (<1 GPa).[18] For tungsten, the diffraction lines (110), (200), (211), (220), (310), (222), and (321) could be detected through the entire range of our measurements. The lattice parameters of W were generally derived from diffraction lines of (110), (200), (211), (220), and (310) using least-squares fitting to a cubic cell. There is no peak overlap among the W, Au, and Be (gasket) diffraction lines. Further experimental details can be found elsewhere.[18]

THEORY

The d spacing from radial x-ray diffraction data was analyzed using the lattice strain theory developed by Singh *et al.*[9–12] According to this theory, the stress state in a polycrystalline sample under uniaxial compression in the diamond anvil cell can be described by a maximum stress along the cell loading axis, σ_3, and a minimum stress in the radial direction, σ_1. The difference between σ_3 and σ_1 is termed the uniaxial stress component or the differential stress t,

$$t=\sigma_3-\sigma_1=2\tau=Y, \tag{1}$$

where τ is the shear strength and Y the yield strength of the sample. The equality in Eq. (1) holds for a Von Mises yield condition and t could be less than the yield strength.

The observed d spacing (d_m) is a function of the angle ψ between the diamond cell loading axis and diffraction plane normal:

$$d_m(hkl)=d_p(hkl)[1+(1-3\cos^2\psi)Q(hkl)], \tag{2}$$

where $d_p(hkl)$ is the d spacing resulting from the hydrostatic component of stress, and

$$Q(hkl)=(t/3)\{\alpha[2G_R(hkl)]^{-1}+(1-\alpha)(2G_V)^{-1}\}. \tag{3}$$

$G_R(hkl)$ is the aggregate shear modulus of grains contributing to the diffraction intensity under the condition of constant stress across grain boundaries (Reuss limit). G_V is the shear modulus under isostrain conditions (Voigt bound).

According to Eq. (2), $d_m(hkl)$ should vary linearly with $1-3\cos^2\psi$. At $\psi=54.7°$ ($1-3\cos^2\psi=0$), the position of the observed x-ray diffraction line reflects the d spacing due to the hydrostatic component of stress, and there is no contribution to the measured d spacing from the differential stress.

The aggregate polycrystalline sample in the diamond anvil cell is generally assumed to be under isostress conditions. In this case, α equals 1 in Eq. (3) and the differential stress can be expressed as:

$$t=6G\langle Q(hkl)\rangle. \tag{4}$$

where $\langle Q(hkl)\rangle$ represents the average $Q(hkl)$ value over all observed reflections, and G is the aggregate shear modulus of the polycrystalline sample. If the differential stress t has reached its limiting value of yield strength at high pressures,

$6\langle Q(hkl)\rangle = t/G$ will reflect the ratio of yield strength to shear modulus.

Upon compression, local deviatoric stresses exist in an aggregate polycrystalline sample due to grain-to-grain strain differences that result in broadening of diffraction lines.[11,21,22] X-ray diffraction peak broadening (β) can also be caused by small grain size. Effects of lattice distortion and grain size on x-ray diffraction peak broadening are well documented elsewhere[41–43] and briefly summarized below.

For angle-dispersive x-ray diffraction, the contributions of small grain size to peak broadening can be expressed by the equation

$$\beta_s = S\lambda/(L\cos\theta), \tag{5}$$

and peak broadening due to the lattice distortion is given by

$$\beta_d = 2\varepsilon\tan\theta, \tag{6}$$

where β_s and β_d represent the grain size and lattice distortion contributions, respectively, S is the Scherrer constant, λ is the x-ray wavelength, L is the average grain size, θ is the Bragg angle, and ε is the microscopic deviatoric strain distribution parallel to the diffraction vector.[43]

In energy-dispersive x-ray diffraction, Bragg's law is expressed by

$$E_x d\sin\theta = hc/2 \tag{7}$$

where E_x is the x-ray photon energy, d is the interplanar spacing, θ is the Bragg angle, h is Planck's constant, and c is the velocity of light. The relation between the peak broadening measured in the angle-dispersive case and that measured in the energy-dispersive case can be obtained through differentiating with respect to 2θ in Eq. (7) (Ref. 32):

$$\delta(E_x) = -[E_x\delta(2\theta)\cot\theta]/2. \tag{8}$$

From Eqs. (5)–(8), we can express the broadening attributed to grain size and lattice distortion in energy dispersive diffraction as

$$\beta_s = Shc/(2L\sin\theta) \tag{9}$$

and

$$\beta_d = \varepsilon E_x. \tag{10}$$

If the energy-dispersive x-ray diffraction peak has a Gaussian profile, the total peak broadening due to grain size and lattice distortion is[24,43]

$$[\beta(E_x)]^2 = [Shc/(2L\sin\theta)]^2 + (\varepsilon E_x)^2. \tag{11}$$

According to Eq. (11), different diffraction peaks should give a linear plot of $[\beta(E_x)]^2$ vs E_x^2 with slope ε^2 and ordinate intercept $[Shc/(2L\sin\theta)]^2$. In this way, we can constrain the microscopic deviatoric strain distribution ε and the average grain size L.[24,43] Taking account of the instrumental broadening $\beta_i(E_x)$, Eq. (11) can be modified as[25,42]

$$[\beta_o(E_x)]^2 - [\beta_i(E_x)]^2 = [Shc/(2L\sin\theta)]^2 + (\varepsilon E_x)^2, \tag{12}$$

where $\beta_o(E_x)$ represents the observed peak broadening.

By using a diffraction pattern from a stress-free sample with a known grain size at ambient conditions the instrumental broadening could be determined. Therefore the average grain size and deviatoric strain distribution can be derived by plotting $[\beta_o(E_x)]^2 - [\beta_i(E_x)]^2$ as a function of E_x^2. Once the deviatoric strain distribution ε is known, the microscopic deviatoric stresses υ can be determined by multiplying by the aggregate Young's modulus E.[22] If the sample is deformed plastically, then this stress also represents the yield strength of the sample, i.e.,

$$\upsilon = \varepsilon E = 2\tau = Y. \tag{13}$$

Under uniaxial loading, both the macroscopic differential stress t and microscopic deviatoric stress υ that the aggregate polycrystalline sample can support are equal to the yield strength ($t=\upsilon=Y$) once plastic deformation is initialed. Thus we have

$$\varepsilon E = 6G\langle Q(hkl)\rangle = Y. \tag{14}$$

The aggregate Young's modulus E can be obtained from the bulk modulus K and shear modulus G using

$$E = 9KG/(3K+G). \tag{15}$$

The bulk modulus can be derived from the hydrostatic compression curve, which can be obtained at $\psi=54.7°$ using radial x-radial diffraction techniques. Therefore, the strength as a function of pressure can be obtained in two ways from the radial x-ray diffraction data. Equations (14) and (15) are strictly true only for elastically isotropic materials and only if both the microscopic deviatoric stress and macroscopic differential stress reach their upper limit (yield strength) in an aggregate polycrystalline sample under uniaxial loading.

RESULTS AND DISCUSSION

Diffraction spectra of the sample were measured to conditions corresponding to a hydrostatic pressure up to 68.8 GPa at room temperature (Fig. 1). Here the pressure is determined using the Au scale[37] from the diffraction data obtained at $\psi=54.7°$. At room temperature, there are some differences in reported equations of state (EOSs) for Au. The recent EOS of Au by Shim *et al.*[37] yields ~3 GPa pressure difference from Anderson *et al.*'s[44] at 60 GPa and room temperature. The shift of diffraction lines for W is larger than for Au. This indicates that W is stronger than Au and can support a larger uniaxial stress.[18] The change of the observed d spacing with direction is caused by the differential stress component $t=\sigma_3-\sigma_1$, which is limited by the yield strength of the material. Gold has a low yield strength, and the uniaxial stress it can support is less than 1 GPa under nonhydrostatic compression to 50 GPa in a diamond cell.[13,14,18] But strong metals like Mo and Re are found to support a differential stress of up to 7 GPa at the same condition.[13,14]

Figure 2 shows plots of d spacing as a function of $1-3\cos^2\psi$ for W (110) diffraction lines at seven pressures. As expected from the theory, our measured d spacings vary linearly with $1-3\cos^2\psi$. The compression curves for tungsten at 54.7° and 0° are shown in Fig. 3. The unit-cell volumes observed at different pressures were fitted to the third-order Birch-Murnaghan equation of state. At $\psi=54.7°$, the

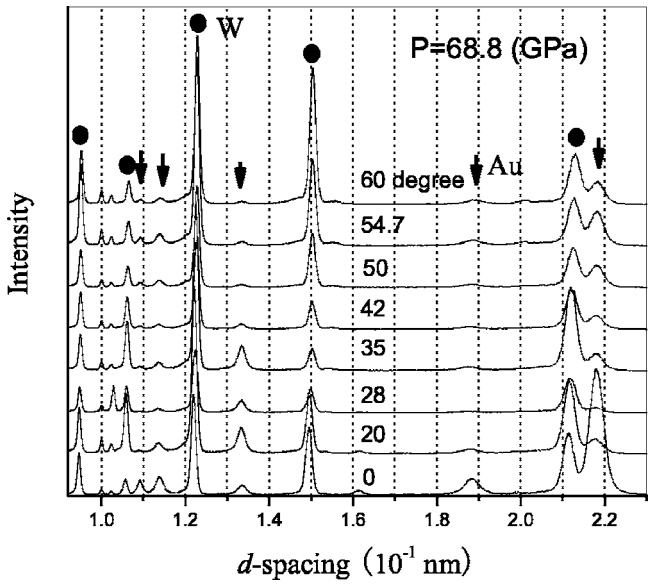

FIG. 1. X-ray diffraction patterns of the sample taken at different ψ under the same loading. The positions of W and Au diffraction peaks are marked by solid circles and arrows, respectively. The pressure is determined from the mean lattice parameter of gold obtained at $\psi=54.7°$.

derived K_0 is 312±36 GPa with K_0' fixed at 4.32, which is the value previously determined from ultrasonic measurements.[27] The bulk moduli obtained from fits of the diffraction data at 0° is 278±9 GPa. Table I summarizes the bulk modulus and its pressure derivative of tungsten from previous experiments and theoretical calculations. The compression curve of tungsten obtained here under uniaxial compression at $\psi=54.7°$ (Fig. 3) is roughly consistent with the reported results from hydrostatic and quasihydrostatic compression data. Pressure-volume states at $\psi=54.7°$ and other main results from this work are summarized in Table II.

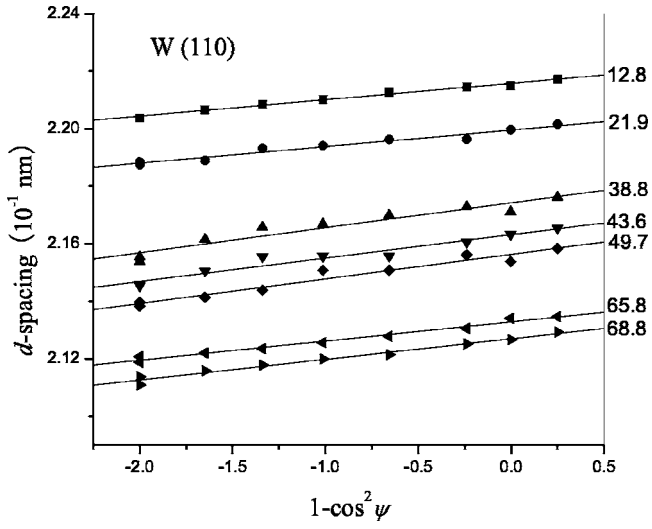

FIG. 2. Dependence of observed d spacing on $1-3\cos^2\psi$ for the tungsten (110) diffraction line at different pressures. The two data points at each pressure step at $\psi=0°$ were obtained at the beginning and completion of the measurements. The solid lines are least-squares fits to the data. The pressures (in GPa) are listed to the right of each line.

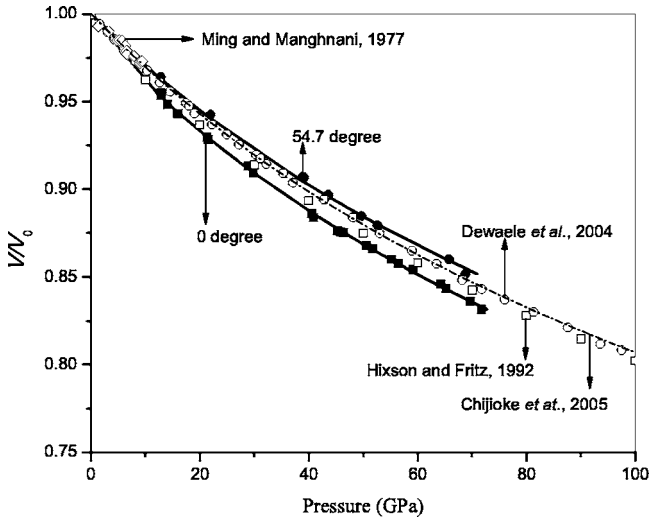

FIG. 3. Compression curves of tungsten from lattice parameters measured at 0° and 54.7°. The pressure is also calculated from the measured diffraction data of gold at 0° and 54.7°. The solid lines are Birch-Murnaghan equation fits to the data at each angle. The open diamonds are the static compression data obtained by Ming and Manghnani from Ref. 29. The open circles are the static compression data of Ref. 7. The open squares and dashed line are the isotherm derived from shock compression data by Ref. 28 and Ref. 8.

The ratio of differential stress to shear modulus ($t/G=6\langle Q\rangle$) is plotted as a function of pressure for tungsten in Fig. 4. The t/G ranges from 0.014 to 0.024 at pressures of 12.8–68.8 GPa with an average value of 0.02. Theoretical calculations indicate that the ideal strength of W corresponds to about 11% of the shear modulus,[31] and thus the high-pressure strength of W remains well below the theoretical limit. Our results for W are comparable to results from radial diffraction studies of other incompressible metals at pressures below 40 GPa: Re ($t/G=0.02$) (Ref. 13) and Mo ($t/G=0.02$) (Ref. 14). Platinum and gold are fcc metals with considerably lower resistance to shear. The t/G values for these materials were found to be 0.03 and 0.007, respectively, at 20 GPa.[13,16] Thus, metals with a wide range of properties exhibit differential stresses that are ~1–3 % of the shear modulus at high pressures. This is much lower than the t/G values (~0.05–0.09) found for oxides and silicates at high pressures.[15,17,18] It is likely that tungsten has already yielded at these pressures, thus the t/G reflects the ratio of yield strength to shear strength (Y/G). The plastic strains are not directly measured in our experiments. Based on finite-element simulations for a similar experimental geometry, it can be estimated that plastic strains are greater than 50% at 70 GPa.[45] Thus, strain hardening is likely to be an important contributor to the strengths.[46]

As discussed above, the deviatoric strain distribution of the polycrystalline W sample can be derived from the energy-dependent peak broadening. Figure 5 shows the square of observed peak broadening (full width at half maximum) against square of energy for five tungsten diffraction

TABLE I. A summary of the bulk modulus (K_0) of tungsten and its pressure derivative ($K_{0'}$) obtained from various methods.

Method	K_0 (GPa)	$K_{0'}$	Reference
Radial XRD (static)	312±36	4.32 (fixed)	This work
Ultrasonic	308.6	4.32	Ref. 27
Ultrasonic	309		Ref. 32
Hydrostatic compression	307±11	4.32 (fixed)	Ref. 29
Quasi-hydrostatic compression	295.2±3.9	4.32±0.11	Ref. 7
Shock compression	280±9	4.32 (fixed)	Ref. 28
Theory	305	3.96	Ref. 30
Theory	331		Ref. 31
Theory	306.5		Ref. 33

lines at the lowest and highest pressures in our experiments. Straight lines with almost the same intercept fit the data very well at two pressures. This indicates that Eq. (12) can be applied to our data and there was no significant change in grain size over our experimental pressure range. We did not observe any systematic difference in peak broadening at different ψ under the same loading.

Figure 6 shows the microscopic deviatoric strain distribution ε of tungsten at different pressures, which was derived from the slope of the lines in Fig. 5. Except for the first pressure step at $P=2.7$ GPa ($\varepsilon=0.0052$), the microscopic deviatoric strain distribution of tungsten is similar ($\varepsilon\approx0.008$) above $\sim$5 GPa. It appears that the microscopic deviatoric strain distribution of tungsten reached the highest value at $P=7.3$ GPa ($\varepsilon=0.0086$), then fell back upon further compression. This may indicate that the tungsten starts to yield at around 7 GPa under nonhydrostatic compression and local deviatoric stresses relaxed due to the plastic flow.

The macroscopic differential stress t can be calculated at each pressure step from Eq. (4) if the shear modulus of tungsten at high pressure is known. By multiplying ε by the aggregate Young's modulus, the microscopic deviatoric stress can also be determined under compression. The single-crystal elastic moduli C_{ij} and their pressure derivatives $\partial C_{ij}/\partial P$ have been measured ultrasonically at 25 °C up to 5 kbar for W.[27] Using these data, the C_{ij} at high pressure were calculated using third-order Eulerian finite-strain equations. The aggregate shear modulus and Young's modulus are derived from the C_{ij} at high pressure. With G and E known, we can calculate both the macroscopic differential stress and microscopic deviatoric stress of tungsten at each pressure step. The results are shown in Fig. 7 and Table II. Also shown in the figure are data obtained from other static compression measurements[1,5] and shock compression.[35,36] It can be seen that the microscopic deviatoric stresses obtained by the analysis of the peak broadening have similar values as the differential stress calculated using the lattice strain theory. It is likely that yield has been achieved for tungsten at high pressures ($P\geqslant\sim7$ GPa), so both the differential stresses and microscopic deviatoric stress are equivalent to yield strength.

Hemley *et al.* investigated the differential stress of tungsten and iron under uniaxial compression using a similar

TABLE II. A list of cell volume (V), differential stress (t), microscopic deviatoric stress (υ), and shear modulus (G) of tungsten at seven pressure steps. The pressure is determined from the mean lattice parameter of gold obtained at $\psi=54.7°$. Cell volume of tungsten is also obtained at $\psi=54.7°$. Shear modulus of tungsten at high pressure are derived using third-order Eulerian finite-strain equations from the data in Ref. 27.

P (GPa)	V (Å^3)	t (GPa)	υ (GPa)	G (GPa)
12.8(0.3)	30.80(0.04)	2.8(0.6)	3.6(0.6)	179
21.9(0.5)	30.11(0.05)	2.6(0.5)	3.7(0.9)	191
38.8(0.3)	28.98(0.05)	5.0(1.4)	4.6(0.6)	214
43.6(0.7)	28.65(0.03)	4.8(0.9)	4.5(0.5)	220
49.7(0.4)	28.27(0.04)	5.2(1.1)	4.9(0.4)	228
65.8(0.8)	27.48(0.06)	4.3(0.7)	5.2(0.3)	248
68.8(0.5)	27.21(0.07)	5.2(1.0)	5.3(0.3)	251

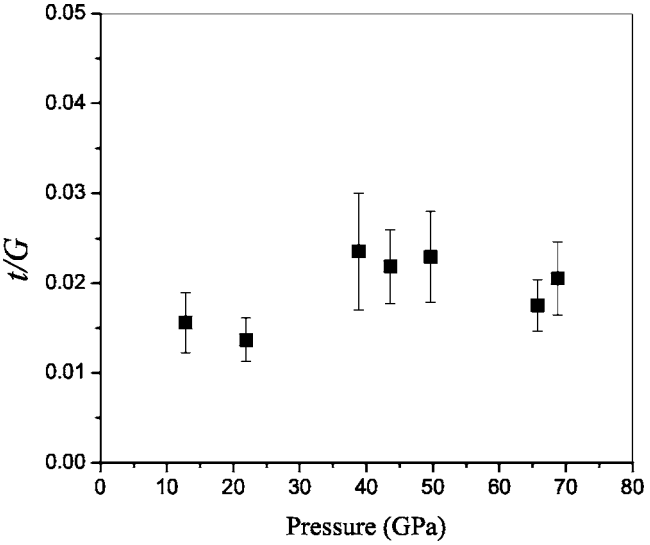

FIG. 4. Ratio of differential stress to shear modulus (t/G) as a function of pressure for tungsten. The pressure is determined from the mean lattice parameter of gold obtained at $\psi=54.7°$. The estimated errors are obtained from the scatter of $d(hkl)$ vs $1-3\cos^2\psi$.

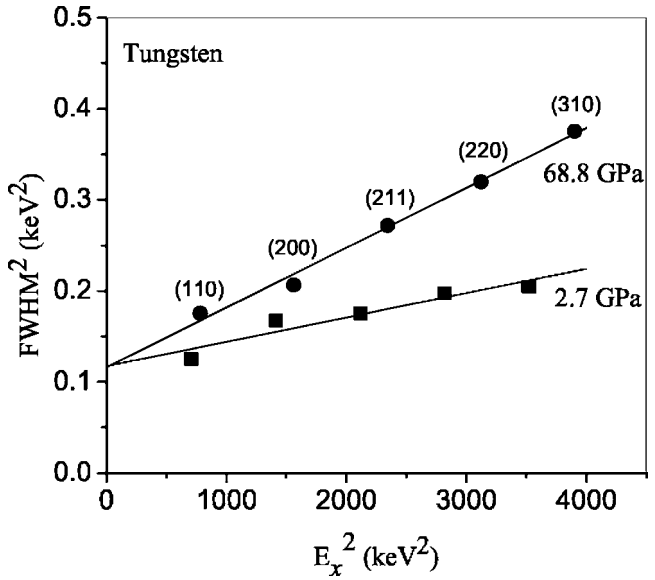

FIG. 5. Energy-dependent peak broadening for tungsten at 2.7 and 68.8 GPa. The solid lines are linear fits to the experimental data. The slope of the straight line reflects the microscopic deviatoric strain distribution of tungsten due to the grain-to-grain contact under compression, and the intercept reflects the grain size and instrumental broadening.

method as ours.[5] It was found that t increases with increasing pressure, reaching values of ~20 GPa for W at 200–300 GPa. At $P=34$ and 74 GPa, the differential stresses they obtained are 4.3 and 4.8 GPa. These results are very consistent with our experiments where both t and v range from 4.3 to 5.3 GPa under pressure between 29.9 and 68.8 GPa. At ultrahigh pressures, the t/G values for W from the data of Ref. 5 are $\sim 0.03 \pm 0.01$, which are consistent with the lower-pressure values obtained here. Bridgman quantitatively measured the shearing stress of various materials at the plastic flow point as a function of pressure up to 5 GPa.[1] The yield strength of W was estimated to be 2.5 GPa at mean

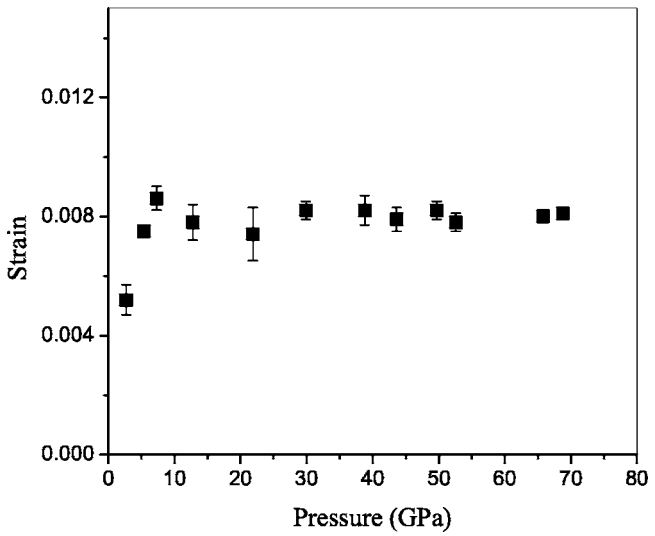

FIG. 6. The microscopic deviatoric strain distribution of tungsten vs pressure.

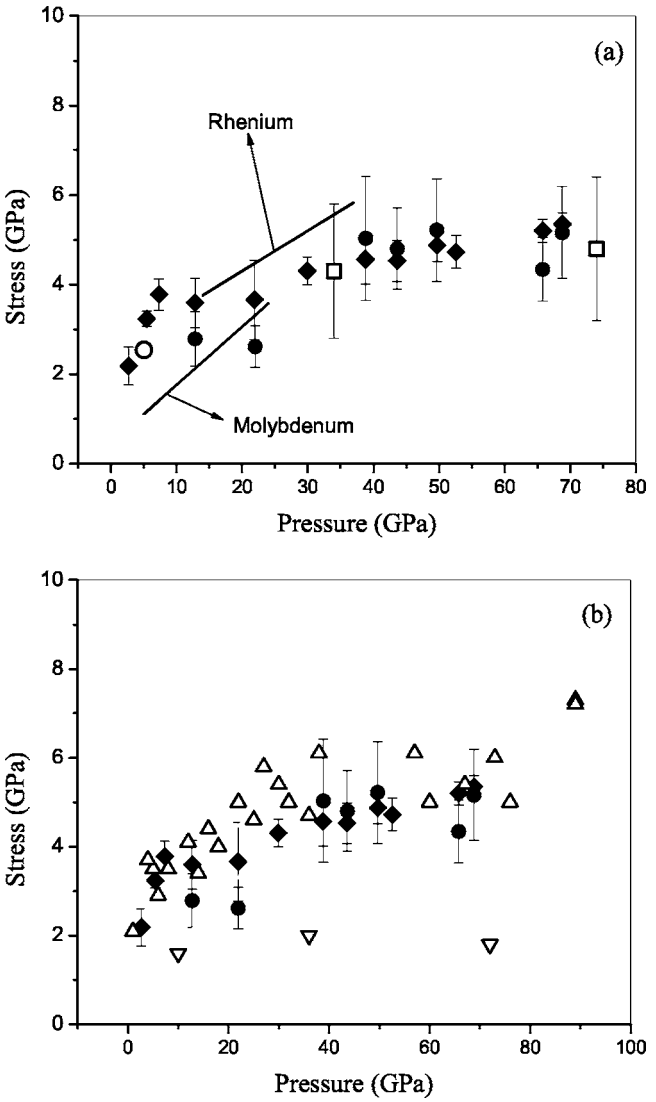

FIG. 7. Differential stress and microscopic deviatoric stress of tungsten as a function of pressure. Other reported yield strength values of tungsten from static compression measurements (a) and shock wave measurements (b) are also shown for comparison. Solid symbols, data from this work (♦ microscopic deviatoric stress and ● differential stress); open symbols, reported data (□ differential stress from Ref. 5; ○ yield strength from Ref. 1; △ isentropic loading from Refs. 35 and 36; ▽ shock loading from Refs. 35 and 36). The solid lines in (a) are the strength vs pressure fitting lines for Re in Ref. 13 and Mo in Ref. 14.

hydrostatic pressures of 5 GPa. The microscopic deviatoric stresses of tungsten from the analysis of peak broadening in our experiments give $v=2.2$ GPa at 2.7 GPa and 3.2 GPa at 5.4 GPa, which are also consistent with Bridgman's data. However, those values may not represent the yield strength of tungsten as the nonhydrostatic pressure below ~7 GPa may not be high enough to deform the sample plastically. Figure 7(a) shows the yield strength of tungsten obtained in this work together with the reported static compression data.[1,5] Also shown in the figure are fitting lines of strength vs pressures for two other incompressible metals: Rhenium, $t=2.5+0.09P$ ($P=14-37$ GPa) (Ref. 13); molybdenum, t

$=0.46+0.13P$ ($P=5-24$ GPa) (Ref. 14). It can be seen that the yield strengths of tungsten determined under static compression are quite consistent, and it has a similar strength as rhenium and molybdenum under uniaxial compression.

Like tungsten, tantalum is an incompressible transition metal with a body centered cubic crystal structure. The yield strength of tantalum has also been reported from static compression studies using either measurements of pressure gradients[45] or diffraction from single crystals.[47] The latter study reported yield strengths of 1.1–3.6 GPa at 36–71 GPa, which are lower than those found here for W. This may in part reflect the lower plastic strains ($\sim 20\%$) achieved in the Ta experiments. In contrast, the pressure gradient measurements yielded values of 4.8–10.3 GPa for relatively low-strain experiments ($\sim 40\%$) at 31–86 GPa with softening at higher compression. For relatively high-strain experiments ($\sim 100\%$), the yield strength values were 3–4 GPa at 35–69 GPa. The latter are more consistent with our measurements for W. Measurements of strength based on pressure gradients suffer from significant uncertainties (e.g., sample thickness) and are valid only under restricted experimental conditions that may be violated due to anvil deformation at higher pressures.

The shear strength of W and W alloys has been measured under shock loading in numerous studies.[26,34–36,48–50] Figure 7(b) shows the yield strengths determined in a study[35,36] using nearly pure W and covering a wide range of shock pressures (to 250 GPa). The yield strengths were constrained from wave profile measurements of shock loading and release paths. The same study also reported yield strengths under quasi-isentropic loading through the use of graded density impactors [Fig. 7(b)]. Quasi-isentropic compression involves slower loading rates and lower temperatures compared with shock loading. As shown in Fig. 7(b), the static yield strength of W determined here from radial x-ray diffraction has roughly the same value as the yield strength under quasi-isentropic loading but considerably higher than those found under shock loading. The constitutive response of materials under static, quasi-isentropic, and shock loading will in general differ due to a variety of factors including strain rate, total strain, temperature, and the details of microstructure development. It is not possible to assess the relative importance of these factors based on the present data. Shock temperatures in W up to 70 GPa are expected to be relatively modest[51] (<515 K) and so it is unlikely that thermal softening alone can explain the low shock strengths compared to static and quasi-isentropic loading. It should also be noted that higher values of yield strength under shock loading have been reported for some W alloys, but the presence of alloying components may have a significant strengthening effect[34] rendering these data incomparable to ours.

Microscopic deviatoric stress exists in a polycrystalline sample under nonhydrostatic compression due to the grain-to-grain contact, especially in a packed powder sample without sintering. Microscopic deviatoric stress will lead to broadening of the diffraction peaks, and measurements of the peak broadening above the yield point, are frequently applied to determining the strength of materials.[21–25] On the other hand, a uniaxial loading system also generates a statistically uniform (macroscopic) differential stress field throughout the sample.[21] In this case, change in d spacing with ψ reflects the response of the shear modulus to the uniaxial stress field. Radial x-ray diffraction techniques together with lattice strain theory have also been used for strength determination for many materials.[13–18] In fact, both of the above two methods are used to determine materials' strength, and should give the same result as both the macroscopic differential stress and microscopic deviatoric stress that the sample can support are equal to the yield strength once the plastic deformation is initialized. Our results as shown in Fig. 7 demonstrate the consistency of these two methods.

CONCLUSION

The yield strength of tungsten under uniaxial compression has been determined to 68.8 GPa from the radial x-ray diffraction data. Results obtained using lattice strain theory and the analysis of the peak broadening are consistent: both t (differential stress) and v (microscopic deviatoric stress) range from 4.3 to 5.3 GPa under pressure between 29.9 and 68.8 GPa. The consistency of the two methods provides confidence in the robustness of strength determination. The strength of tungsten obtained in this work is also compared with the reported data from the static compression and shock wave (quasi-isentropic loading) experiments. The static strength of tungsten is considerably larger than previous values reported under shock compression at these pressures, but comparable to values inferred from quasi-isentropic compression experiments.

ACKNOWLEDGMENTS

The authors thank J. Z. Hu for experimental assistance, and A. Kubo, S. R. Shieh, and B. Kiefer for helpful discussion. Financial support was provided by NSF EAR and the Carnegie-DOE Alliance Center (C-DAC). C-DAC is funded by the Department of Energy through the Stewardship Sciences Academic Alliance Program under Grant No. DE-FC03-03NA00144. Experiments were carried out at beamline X17C of the National Synchrotron Light Source, Brookhaven National Laboratory. X17C is supported by the NSF and DOE.

*Author to whom correspondence should be addressed. Electronic address: duanweihe@yahoo.com

[1] P. W. Bridgman, Phys. Rev. **48**, 825 (1935).
[2] P. W. Bridgman, Rev. Mod. Phys. **17**, 3 (1945).
[3] P. W. Bridgman, Rev. Mod. Phys. **18**, 1 (1946).
[4] N. E. Christensen, A. L. Ruoff, and C. O. Rodriguez, Phys. Rev. B **52**, 9121 (1995).
[5] R. J. Hemley, H. K. Mao, G. Shen, J. Badro, P. Gillet, M. Hanfland, and D. Hausermann, Science **278**, 1242 (1997).
[6] H. K. Mao, P. M. Bell, J. W. Shaner, and D. J. Steinberg, J. Appl. Phys. **49**, 3276 (1978).
[7] A. Dewaele, P. Loubeyre, and M. Mezouar, Phys. Rev. B **70**, 094112 (2004).
[8] A. D. Chijioke, W. J. Nellis, and I. F. Silvera, J. Appl. Phys. **98**, 073526 (2005).
[9] A. K. Singh, J. Appl. Phys. **73**, 4278 (1993).
[10] A. K. Singh and C. Balasingh, J. Appl. Phys. **75**, 4956 (1994).
[11] A. K. Singh, H. K. Mao, J. Shu, and R. J. Hemley, Phys. Rev. Lett. **80**, 2157 (1998).
[12] A. K. Singh, C. Balasingh, H. K. Mao, R. J. Hemley, and J. Shu, J. Appl. Phys. **83**, 7567 (1998).
[13] T. S. Duffy, G. Shen, D. L. Heinz, J. Shu, Y. Ma, H. K. Mao, R. J. Hemley, and A. K. Singh, Phys. Rev. B **60**, 15063 (1999).
[14] T. S. Duffy, G. Shen, J. Shu, H. K. Mao, R. J. Hemley, and A. K. Singh, J. Appl. Phys. **86**, 6729 (1999).
[15] S. R. Shieh, T. S. Duffy, and B. S. Li, Phys. Rev. Lett. **89**, 255507 (2002).
[16] A. Kavner and T. S. Duffy, Phys. Rev. B **68**, 144101 (2003).
[17] S. R. Shieh, T. S. Duffy, and G. Shen, Phys. Earth Planet. Inter. **143–44**, 93 (2004).
[18] D. He, S. R. Shieh, and T. S. Duffy, Phys. Rev. B **70**, 184121 (2004).
[19] A. K. Singh and T. Kenichi, J. Appl. Phys. **90**, 3269 (2001).
[20] S. Merkel, H. R. Wenk, J. F. Shu, G. Y. Shen, P. Gillet, H. K. Mao, and R. J. Hemley, J. Geophys. Res. **107**, 2271 (2002).
[21] D. J. Weidner, Y. Wang, and M. T. Vaughan, Geophys. Res. Lett. **21**, 753 (1994).
[22] D. J. Weidner, Y. Wang, and M. T. Vaughan, Science **266**, 419 (1994).
[23] D. J. Weidner, L. Li, M. Davis, and J. H. Chen, Geophys. Res. Lett. **31**, L06621 (2004).
[24] J. Chen, D. J. Weidner, and M. T. Vaughan, Nature (London) **419**, 824 (2002).
[25] J. Zhang, L. Wang, D. J. Weidner, T. Uchida, and J. Xu, Am. Mineral. **87**, 1005 (2002).
[26] J. S. Hua, F. Q. Jing, H. Tan, and S. L. Hu, J. Phys.: Condens. Matter **14**, 10843 (2002).
[27] K. W. Katahara, M. H. Manghnani, and E. S. Fisher, J. Phys. F: Met. Phys. **9**, 773 (1978).
[28] R. S. Hixson and J. N. Fritz, J. Appl. Phys. **71**, 1721 (1992).
[29] L. C. Ming and M. H. Manghnani, J. Appl. Phys. **49**, 208 (1978).
[30] Y. Wang, D. Chen, and X. Zhang, Phys. Rev. Lett. **84**, 3220 (2000).
[31] D. Roundy, C. R. Krenn, M. L. Cohen, and J. W. Morris, Philos. Mag. A **81**, 1725 (2001).
[32] F. H. Featherston and J. R. Neighbours, Phys. Rev. **130**, 1324 (1963).
[33] A. L. Ruoff, C. O. Rodriguez, and N. E. Christensen, Phys. Rev. B **58**, 2998 (1998).
[34] J. C. F. Millett, N. K. Bourne, Z. Rosenberg, and J. E. Field, J. Appl. Phys. **86**, 6707 (1999).
[35] L. C. Chhabildas, J. R. Asay, and L. M. Barker, Sandia National Laboratory Report No. SAND88-0306.UC-34, 1988 (unpublished).
[36] L. C. Chhabildas and J. R. Asay, in *Shock-Wave and High-Strain-Rate Phenomena in Materials*, edited by M. A. Meyers, L. E. Murr, and K. P. Staudhammer (Marcel Dekker, New York, 1992), pp. 947–955.
[37] S.-H. Shim, T. S. Duffy, and T. Kenichi, Earth Planet. Sci. Lett. **203**, 729 (2002).
[38] J. Z. Hu, H. K. Mao, Q. Z. Guo, and R. J. Hemley, in *Science and Technology of High Pressure: Proceedings of AIRAPT-17*, edited by M. H. Manghnani, W. J. Nellis, and M. F. Nicol (Universities Press, Hyderabad, India, 2000), pp. 1039–1042.
[39] E. M. Gullikson, in *X-ray Data Booklet*, edited by A. C. Thompson and D. Vaughan (University of California Press, Berkeley, CA, 2001).
[40] M. R. Daymond and M. W. Johnson, J. Appl. Crystallogr. **34**, 263 (2001).
[41] H. P. Klug and L. E. Alexander, *X-Ray Diffraction Procedures* (Wiley, New York, 1974).
[42] B. Warren, *X-Ray Diffraction* (Addison-Wesley, London, 1989).
[43] L. Gerward, S. Morup, and H. Topsoe, J. Appl. Phys. **47**, 822 (1976).
[44] O. L. Anderson, D. G. Isaak, and S. Yamamoto, J. Appl. Phys. **65**, 1534 (1989).
[45] S. T. Weir, J. Akella, C. Ruddle, T. Goodwin, and L. Hsiung, Phys. Rev. B **58**, 11258 (1998).
[46] N. Nishiyama, Y. B. Wang, T. Uchida, T. Irifune, M. L. Rivers, and S. R. Sutton, Geophys. Res. Lett. **32**, L04307 (2005).
[47] A. Dewaele and P. Loubeyre, Phys. Rev. B **72**, 134106 (2005).
[48] M. Zhou and R. J. Clifton, J. Appl. Mech. **64**, 487 (1997).
[49] J. R. Asay, L. C. Chhabildas, and D. P. Dandekar, J. Appl. Phys. **51**, 4774 (1976).
[50] D. P. Dandekar, J. Appl. Phys. **47**, 4703 (1976).
[51] J. X. Peng, F. Q. Jing, D. H. Li, and L. L. Wang, J. Appl. Phys. **98**, 013508 (1976).